J|A|C|S
ARTICLES
Published on Web 11/08/2003

# Circular Dichroism Imaging Microscopy: Application to Enantiomorphous Twinning in Biaxial Crystals of 1,8-Dihydroxyanthraquinone

Kacey Claborn, Eileen Puklin-Faucher, Miki Kurimoto, Werner Kaminsky,* and Bart Kahr*

*Contribution from the Department of Chemistry, Box 351700, University of Washington, Seattle, Washington 98195-1700*

Received April 15, 2003; E-mail: kahr@chem.washington.edu

***Abstract:*** A microscope was constructed for imaging circular dichroism of heterogeneous anisotropic media. To avoid linear biases that are common with electronic circular polarization modulation, we chose a retrogressive solution: mechanical light modulation by rotating a linear polarizer with respect to a quarter wave plate continuously tuned by tilting to the operating wavelength. Our comparatively slow technique succeeds with near-perfect circular input and signal averaging using a CCD camera. We have applied the method to anomalously birefringent crystals of 1,8-dihydroxyanthraquinone that are shown to have intergrown mirror image domains, undetected by X-ray diffraction because the twinning complexity renders differences in anomalous dispersion, already small, unreliable. The origin of the anomalous birefringence and the assignment of the absolute configuration are discussed.

## Introduction

For generations, measurements of chiroptical effects (circular dichroism (CD) or optical rotation) of organized media have foundered on much larger linear anisotropies that otherwise disappear in isotropic solutions.[1,2] Here, we describe the construction of a circular dichroism imaging microscope (CDIM) that we have used to reveal heterochiral domains in biaxial dye crystals. Such heterogeneity is typically masked by linear birefringence (LB) and linear dichroism (LD) and is invisible by conventional X-ray scattering. Contrast in optical microscopy based upon CD is likely to have many applications in crystallography as well as in cell biology and pathology where organized, optically active structures are ubiquitous.

The idea of a CD microscope for anisotropic samples is not new. In 1982, Maestre and Katz adapted a Cary spectropolarimeter to a microscope[3] for single point measurements of the CD spectra of chromatin. They encountered instrumental artifacts[4] arising from electronic polarization modulators in commercial instruments that typically generate sinusoidally varying polarization states,[5] thereby introducing a small admixture of linearly polarized light into the circularly polarized output. Residual ellipticity, when coupled with the LB and LD of ordered media, generates artifactual CD signals.[6,7] Strain in photoelastic modulators (PEMs) compounds these artifacts.[8] Attempts have been made to skirt these problems by adding additional modulators,[9] rotating the sample,[10] and performing complex analytical transformations of independent chiroptical measurements.[11] Most recently, Kuroda, in collaboration with JASCO, made advances by tailoring a single point CD spectropolarimeter for solid-state samples by selecting a photomultiplier tube with the smallest polarization bias and a PEM with the least residual static birefringence.[12] We chose a different tack, eschewing electronic polarization modulation to avoid imperfections in our circular polarization, while at the same time making CD images.

(1) Michl, J.; Thulstrup, E. W. *Spectroscopy with Polarized Light*, VCH: New York, 1986.
(2) Important exceptions include the extensive work on the CD of nematic liquid crystals by Kuball and co-workers (See: Kuball, H.-G.; Höfer, T. In *Circular Dichroism: Principles and Applications*, 2nd ed.; Berova, N., Nakanishi, K., Woody, R. W., Eds.; Wiley-VCH: New York, 2000; pp 133−158), the analysis of uniaxial crystals of coordination compounds by Mason and Kuroda (See: Kuroda, R. In *Circular Dichroism: Principles and Applications*, 2nd ed.; Berova, N., Nakanishi, K., Woody, R. W., Eds.; Wiley-VCH: New York, 2000; pp 159−184), and studies of oriented membranes by Huang and co-workers (See: Wu, Y.; Huang, H. W.; Olah, G. *Biophys. J.* **1990**, *57*, 797−806). Studies of optical rotation in orienting media include the HAUP (high accuracy universal polarimetry) method of Kobayashi and co-workers (See: Kobayashi, J.; Uesu, Y. *J. Appl. Crystallogr.* **1983**, *16*, 204−211. Kobayashi, J.; Uesu, Y.; Takehara, H. *J. Appl. Crystallogr.* **1983**, *16*, 212−219), and its variants (See: Kaminsky, W. *Rep. Prog. Phys.* **2000**, *63*, 1575−1640).
(3) Maestre, M. F.; Katz, J. E. *Biopolymers* **1982**, *21*, 1899−1908. See also: Maestre, M. F.; Salzman, G. C.; Tobey, R. A.; Bustamante, C. *Biochemistry* **1985**, *24*, 5152−5157. Livolant, F.; Mickols, W.; Maestre, M. F. *Biopolymers* **1988**, *27*, 1761−1769. Livolant, F.; Maestre, M. F. *Biochemistry* **1988**, *27*, 3056−3068.
(4) Shindo, Y.; Nishio, M.; Maeda, S. *Biopolymers* **1990**, *30*, 405−413. Shindo, Y.; Ohmi, Y. *J. Am. Chem. Soc.* **1985**, *107*, 91−97.
(5) Hipps, K. W.; Crosby, G. A. *J. Phys. Chem.* **1979**, *83*, 555−562.
(6) Schellman, J.; Jensen, H. P. *Chem. Rev.* **1987**, *87*, 1359−1399.
(7) Disch, R. L.; Sverdlik, D. I. *Anal. Chem.* **1969**, *41*, 82−86.
(8) Nordén, B. *Acta Chem. Scand.* **1972**, *26*, 1763−1776. Davidsson, Å.; Nordén, B. *Spectrochim. Acta, Part A* **1976**, *32*, 717−722. Davidsson, Å; Nordén, B.; Seth, S. *Chem. Phys. Lett.* **1980**, *70*, 313−316.
(9) Cheng, J. T.; Nafie, L. A.; Stephens, P. J. *J. Opt. Soc. Am.* **1987**, *65*, 1031−1035.
(10) Tunis-Schneider, M. J. B.; Maestre, M. F. *J. Mol. Biol.* **1970**, *52*, 521−541. Nuckolls, C.; Katz, T. J.; Verbiest, T.; Van Elshocht, S.; Kuball, H.-G.; Kiesewalter, S.; Lovinger, A. J.; Persoons, A. *J. Am. Chem. Soc.* **1998**, *120*, 8656−8660.
(11) Kuball, H.-G.; Altschuh, J. *Chem. Phys. Lett.* **1982**, *87*, 599−603.
(12) Kuroda, R.; Harada, T.; Shindo, Y. *Rev. Sci. Instrum.* **2001**, *72*, 3802−3810.

## Circular Dichroism Imaging Microscope

**Theory.** Reasonable sensitivity in CD measurements is commonly achieved by rapid sampling concomitant with electronic light modulation at rates of 50−100 kHz. Why then not add contemporary CCD detection to make CD images? Operating at less than 1 kHz, CCDs are incompatible with PEMs. While others are trying to force compatibility[13] by speeding up the CCD[14] or slowing down the modulation,[15] these designs remain constrained by limited spectral ranges, noise, and parasitic ellipticities.[16] On the other hand, physicists recently built single point CD spectropolarimeters for anisotropic media via schemes using mechanical light modulation with photomultiplier tubes as detectors.[17] Their devices were extremely slow but nevertheless suited to large, homogeneous, strong circularly dichroic crystals.

We built a circular dichroism imaging microscope (CDIM) based on the apparently retrogressive mechanical modulation of near perfect circularly polarized light (CPL), akin to the original procedure of Cotton,[18] in conjunction with charge coupled device (CCD) detection. Signal-to-noise lost in slow modulation (<30 Hz) is regained by signal averaging with a CCD camera. We abandoned the use of a broad band $\lambda/4$ plate in favor of a variable retarder that is tilted so as to function as a perfect $\lambda/4$ plate at each wavelength.

The Jones matrix for a birefringent and circularly dichroic sample (neglecting linear absorption) is[6]

$$j_{\delta,\eta} = \begin{bmatrix} e^{ix} & i\eta\,\dfrac{\sin x}{x} \\ -i\eta\,\dfrac{\sin x}{x} & e^{-ix} \end{bmatrix}$$

where $x = \delta/2$ ($\delta = 2\pi\Delta nL/\lambda$ is the phase shift of the extraordinary and ordinary rays exiting the sample) and $\Delta n$ is the linear birefringence (LB). The CD is defined as $4\eta = (I_+ - I_-)/I_o \equiv \eta'$, where $I_+$ and $I_-$ are right and left CPL, respectively. The complex vectors $A$ represent these light forms, where $E_0$ is the amplitude of the incoming light wave:

$$A = \frac{1}{\sqrt{2}}\begin{bmatrix} 1 \\ \pm i \end{bmatrix} E_0$$

The intensity $I_\pm'$ is found from $A_\pm'^{*} \cdot A_\pm'$, where $A_\pm' = j_{\delta,\eta} \cdot A_\pm$. The total intensity is then

$$\frac{I_\pm'}{E_0^2} = 1 \pm 2\eta\,\frac{\sin x \cos x}{x} + \eta^2\,\frac{\sin^2 x}{x^2}$$

The normalized intensity difference in a birefringent sample is found as

$$\frac{I_+' - I_-'}{I_0} = 4\eta\,\frac{\sin x \cos x}{x} = \eta'\,\frac{\sin \delta}{\delta}$$

This expression describes the observed CD in a birefringent sample provided that there is no parasitic linearly polarized contribution to the incoming CPL.

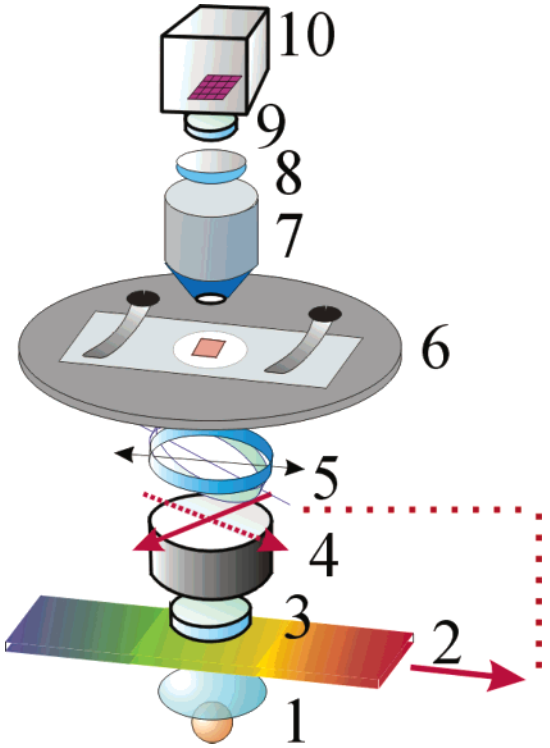


***Figure 1.*** Visible light circular dichroism imaging microscope (CDIM). Schematic omits motors and mounts. (1) Light source, (2) variable interference filter, (3) depolarizer, (4) rotating polarizer, (5) tilting $\lambda/4$-compensator, (6) sample mount, (7) objective, (8) projector lens, (9) depolarizer, (10) CCD-camera.

**Experimental.** A depolarizer, sliding interference filter, Glan Thompson polarizer fixed to a gear driven by a stepper motor, and tilting $\lambda/4$ plate were mounted beneath the sample stage of a microscope (Figure 1). To obtain CD measurements on oriented samples, the polarizer is alternately driven to +45° and −45° with respect to the extinction directions of a $\lambda/4$ retarder that is tuned by tilting about an axis perpendicular to the light path to compensate for dispersion. Tilting the retarder changes the elliptic cross section traversed by the incident light and thereby the effective birefringence of the retarder. This ensures the integrity of alternating right and left CPL produced at all wavelengths selected by the variable interference filter. The difference of the two images, normalized by the regular absorption of the sample, yields the uncorrected CD per pixel in terms of $(I_{45°} - I_{-45°})/I_o$. After the integrated data is stored, the interference filter is advanced to another wavelength and the $\lambda/4$-compensator is adjusted accordingly. To obtain a CD spectrum of a heterogeneous sample, a region as small as a few pixels of a 640 × 480-pixel image is compared to a reference area showing no CD. The difference between the sample and reference regions, each normalized to the number of pixels, is then plotted versus the wavelength between 380 and 700 nm. Such comparisons, independent of light fluctuations, increase accuracy. We routinely integrate many images before calculating the difference to reduce the noise level. A background image

(13) Stenflo, J. O.; Povel, H. A. *Appl. Opt.* **1985**, *24*, 3983−3898. Povel, H. *Opt. Eng.* **1995**, *34*, 1870−1878.
(14) Povel, H.; Aebersold, H.; Stenflo, J. O. *Appl. Opt.* **1990**, *29*, 1186−1190.
(15) Andert, K.; Schälike, W.; Nölting, B.; Pittelkow, R.; Wetzel, R.; Snatzke, G. *Rev. Sci. Instrum.* **1991**, *62*, 1912−1915.
(16) Bobbitt, D. R. In *Analytical Applications of Circular Dichroism*; Purdie, N., Brittain, H. G., Eds.; Elsevier: New York, 1994.
(17) Moxon, J. R. L.; Renshaw, A. R. *J. Phys.: Condens. Matter* **1990**, *2*, 6807−6836. Kremers, M.; Meekes, H. *J. Phys. D: Appl. Phys.* **1995**, *28*, 1212−1224.
(18) Cotton rotated a Fresnel rhomb. See: Cotton, A. *Ann. Chim. Phys.* **1896**, *8*, 347−432.

obtained from a measurement without the sample is subtracted from the final image. In this way, we reproduced the Cotton effects associated with crystalline $NiSO_4 \cdot 6H_2O$ along the optic axis.[17,19]

We used a linear polarizer to calibrate the tunable $\lambda/4$ plate. When a CD image is recorded, no signal is obtained when the polarizer (**4** in Figure 1) is ideally aligned between the eigenrays of a $\lambda/4$ retarder that is optimized for that wavelength. As we vary the wavelength with the interference filter, we adjust the tilt angle until no signal is measured. The signal varied smoothly over the angular changes applied to polarizer and compensator positions. The zero crossing of the signal was used to automatically calibrate the optical components.

All polarizing and refracting components of a Prior Scientific microscope (200-MP3500KT) were removed before coupling with a C-mount to a COHU CCD camera (4910 Series). The microscope was equipped with a monochromator system consisting of a linear interference filter (Reynard Corp., model R04610-00), which in combination with a variable slit limits the spectral line width to 10 nm in the range of 380−700 nm. The $\lambda/4$ retarder is a low order birefringent plate. A video card that supports Video For Windows format reads the output of the camera. The driver for the microscope was written in Delphi. Additional software packages used were "TVicHW32 5.0"[20] to address the parallel printer port, and the commercial drivers for the Osprey video card.[21] The motors are driven via custom electronics through the parallel printer port of the PC.

### Linear Anisotropies

Linear anisotropies were analyzed with a prototype of the MetriPol System now available from Oxford Cryosystems.[22] By modulating the intensity signal as a function of the polarizer angle α, $I/I_o(\alpha)$ for each pixel is subject to a Fourier separation of the disparate optical contributions that are displayed in false color images representing the overall transmission, the phase factor $\delta$, and the directions of the eigenrays, also called extinction.[23] The expression for transmitted intensity follows:

$$\frac{I}{I_o} = \frac{1}{2}[1 + \sin^2(\alpha - \varphi)\sin\delta]$$

where $\varphi$ is the orientation of the slow vibration direction as measured counterclockwise from the horizontal axis.

To implement the MetriPol method, another Prior Scientific microscope (200-MP3500KT) was adapted with a stepper motor driven rotating polarizer, circular analyzer consisting of a linear analyzer and $\lambda/4$ plate aligned at 45°, and an 8-bit monochrome CCD digital camera. The 610 nm illumination was accessed with an interference filter. The measurements were calibrated for a linear camera response, $\lambda/4$ plate alignment, and polarization bias of the light source, camera, and objective. Image sensitivity is ∼0.1% of the transmission, 0.05 nm of the retardation $L\Delta n$, and ∼0.1° of the orientation.

(19) Harada, T.; Shindo, Y.; Kuroda, R. *Chem. Phys. Lett.* **2002**, *360*, 217−222.
(20) Victor Ishikeev: http://www.enytechtaiwan.com/tools.htm, 2001.
(21) View Cast Corporation: http://www.mmac.com/.
(22) http://www.metripol.com/.
(23) Glazer, A. M.; Lewis, J. G.; Kaminsky, W. *Proc. R. Soc. London, Ser. A* **1996**, *452*, 2751−2765.

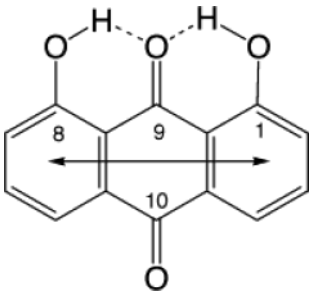


***Figure 2.*** 1,8-Dihydroxyanthraquinone (**DHA**) with the electric dipole transition moment indicated for the lowest energy $\pi \rightarrow \pi^*$ transition.[40]

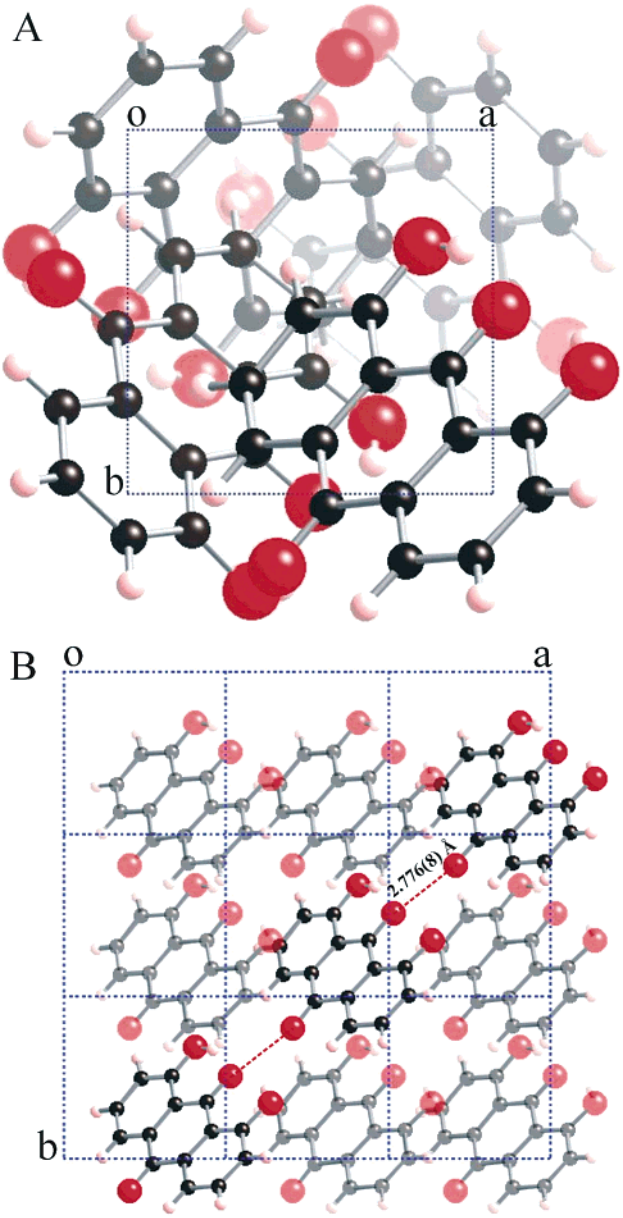


***Figure 3.*** (A) Unit cell of the $P4_1$ crystal viewed along the four-fold axis [001]. (B) Single layer of **DHA**. In (A), the shading indicates depth. In (B), all of the molecules are at the same height. Here, the highlighting serves merely to emphasize one dipole-coupled chain within a layer.

### Crystal Structure

To demonstrate the viability of CD microscopy, we chose as a first sample crystalline 1,8-dihydroxyanthraquinone (**DHA**, Figure 2). Large (0.5 cm × 0.5 cm × 100 $\mu$m), square, orange

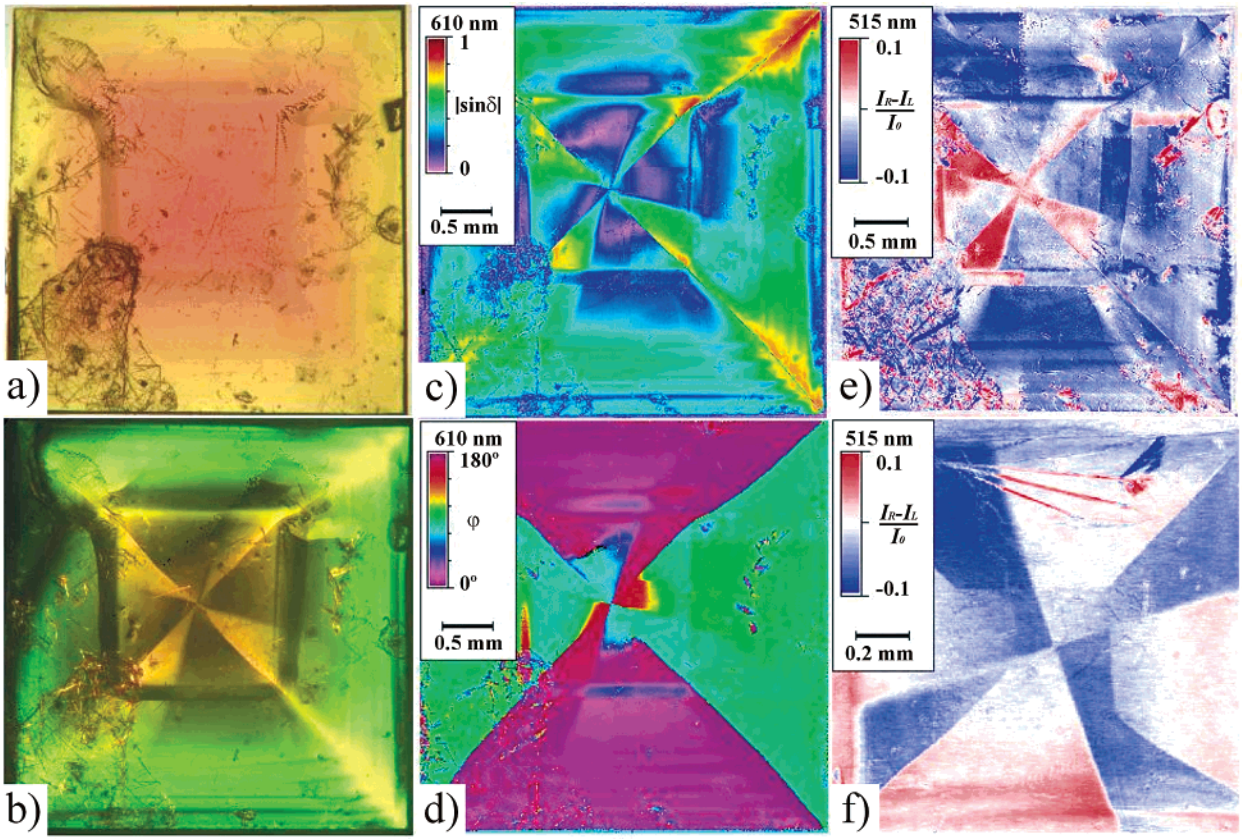


***Figure 4.*** (a) **DHA** crystal (2.5 mm × 2.5 mm × 100 $\mu$m) in white light viewed along [001]. The absorbance is larger in the raised center. (b) Crystal in (a) between crossed polarizers. When viewed along [001], the presumed optic axis, the crystal is not wholly extinct. (c) Linear birefringence image recorded as the sine of the retardance, $\delta = 2\pi\Delta nL/\lambda$, at 610 nm. (d) Orientation of the optical indicatrix recorded as the extinction angle from the horizontal axis in degrees. (e) Circular dichroism image of the crystal in (a−d) recorded as $(I_R - I_L)/I_o$ at 515 nm. (f) Circular dichroism of the center of another crystal with a heterochiral pinwheel.

plates were formed by evaporation of 50:50 (v:v) acetone/acetonitrile solutions. The crystals were often raised in the center and along the borders between lateral growth sectors as seen in the optical density in Figure 4a, but were nevertheless well suited to optical experiments as grown.

The crystal structure of **DHA** was determined previously.[24] The molecules crystallize in the enantiomorphous space groups $P4_{1(3)}$. As such, they must occupy general positions in the lattice but nevertheless have near $C_{2v}$ symmetry by virtue of the fact that the hydroxyl hydrogen atoms are intramolecularly bound to the oxygen at position 9, thus creating a rigid, flat, pentacyclic structure. Four molecules in the unit cell spiraling along [001] are pictured in Figure 3A. The molecules form lamellae with close packing between aromatic molecules of ∼3.5 Å. The strongest interactions between molecules appear to be of the dipole−dipole type, with polar chains of carbonyl oxygen atoms making $O_9 \cdot\cdot O_{10}$ contacts between molecules of 2.776(8) Å (Figure 3B). A gas-phase dipole moment of 0.98 D, negative in the direction of the tri-oxygen side of the molecular polar axis, was calculated using Spartan[25] at the HF 6-31G* level of theory. Nevertheless, the interactions between molecules are not strongly determined. We have found two additional polymorphs of **DHA** characterized by very different packing modalities that will be described in a forthcoming report.

(24) Jagannadham, A. V. *Z. Kristallogr.* **1957**, *108*, 457−458. Prakash, A. *Z. Kristallogr.* **1965**, *122*, 272−282.
(25) *PC Spartan Pro, Version 1.0.3*; Wave function Inc., Irvine, CA, 2000.

## Anomalous Linear Birefringence

**DHA** was selected for this study in part because it has long been a thorn in our side. We studied this crystal in the context of a review of so-called "optically anomalous crystals".[26] Despite the clearly tetragonal morphology and X-ray crystal structure, the crystals seemed to show pronounced LB when viewed along [001], the direction that should be the optic axis,[27] and complex extinction patterns.

Extensive studies were directed at the origin of the optical desymmetrization. Many optically anomalous molecular crystals owe their peculiar physical properties to the presence of impurities or disordered molecules that are distributed non-statistically and thus break the symmetry.[28] We could find no such impurities or minor orientations in difference Fourier maps. We considered the possibility that an invisible impurity might be a tautomer,[29] but could not find one by solid-state $^1$H or $^{13}$C NMR nor equilibrate the crystals thermally or photochemically to thereby obtain optical homogeneity.

Because CD varies as $(\sin\delta)/\delta$, the phase factor $\delta$ must be quantified to derive the absolute CD. This was done using the

(26) Kahr, B.; McBride, J. M. *Angew. Chem., Int. Ed. Engl.* **1992**, *31*, 1−26.
(27) The curious observation was first reported by: Neuhaus, A. *Z. Kristallogr.* **1943**, *105*, 195.
(28) Vaida, M.; Shimon, L. J. W.; Weisinger-Lewin, Y.; Frolow, F.; Lahav, M.; Leiserowitz, L.; McMullan, R. K. *Science (Washington, DC)* **1988**, *241*, 1475−1479. McBride, J. M.; Bertman, S. B. *Angew. Chem., Int. Ed. Engl.* **1989**, *28*, 330−333.
(29) Smulevich, G.; Marzocchi, M. P. *Stud. Biophys.* **1984**, *104*, 105−110; *Chem. Phys.* **1985**, *94*, 99−108; *Chem. Phys.* **1986**, *105*, 159−171.

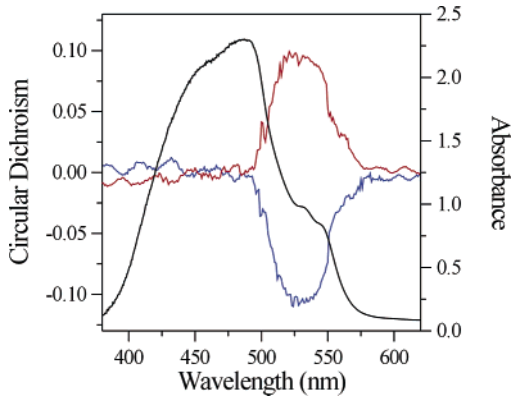


***Figure 5.*** Electronic absorption (black) and circular dichroism spectra (red and blue) of a **DHA** crystal corresponding to the red and blue regions in Figure 4e, respectively. CD is expressed at the ratio $(I_R - I_L)/I_o$. Absorbance at $\lambda_{max}$ in this sample is quite high at nearly 2.5, but identical spectra were made from samples with absorbance less than 1. As one approaches absorbances of 3, the CDIM is limited by a lack of transmitted light.

rotating polarizer technique. The crystals had a variable $|\sin \delta|$, showing the largest birefringence at growth sector boundaries (Figure 4c). Curiously, in the center of the crystal, two distinct pinwheels were evident, having values of $\sin(\delta)$ that alternated between regions with maximum values of 0.25 to about 0.60 (Figure 4c). The crystals showed great variance in their eigenray directions (described by the extinction angle $\varphi$ in Figure 4d). While the optical indicatrices of the (100) and (010) growth sectors were clearly related to one another more or less by 90° rotations around [001], there were marked deviations from orthogonality especially in the center of the crystals. Images produced between crossed polarizers or with the rotating polarizer method[23] could reflect ellipticity changes that result from CD (see below) as well as LB.

### Circular Dichroism Microscopy

Stress resulting from twinning could in principle account for the anomalous birefringence, but we could not detect any such twinning in Laue patterns. Only pernicious enantiomorphous twinning could so go unnoticed. We therefore examined the crystals under the CDIM.

The crystals absorbed light at 490 nm[30] (Figure 5) as compared to 426 nm ($1.2 \times 10^4$ L mol$^{-1}$ cm$^{-1}$) in acetonitrile solution. The crystal spectrum also showed a low-energy shoulder at ~530 nm that was not present in the solution spectrum. The LD was vanishingly small for light incident on the plate face.

No contrast was seen in the CDIM at 490 nm. On the other hand, micrographs recorded at 515 nm dramatically show mirror image domains as red (CD is positive) and blue (CD is negative) heterochiral pinwheels (Figure 4e and f). Blue pinwheels always point counterclockwise and red pinwheels always point clockwise, indicating that the crystals tended to grow predominantly along one direction of the polar [001] axis. These images are independent of sample rotation. This is the surest way to rule out linear biases in the optical train. As seen in spectra in Figure 5, the CD is only associated with the low-energy shoulder of the absorption band.

(30) Crystal absorption spectra were obtained with SpectraCode Multipoint Absorbance Imaging (MAI-20) microscope.

An obvious twinning mechanism involves an orientational disorder in which a molecule flipped 180° about its long anthraquinone axis begins the switch of a right-handed helix into a left-handed helix or vice versa. Hydroxyl groups would argue against disorder but they are insulated through intramolecular H-bonds, and therefore they have an unexpectedly small role in determining the crystal packing.

The twin law pictured in Figures 4e and f that leads to pinwheels is only one of several enantiomorphous twins laws in **DHA**. Other twin planes include (100), (001), as well as (110) without pinwheels. The (100) and (110) twin planes are seen more clearly in Figure 6. Region c is related to the nucleation of a crystal layer that would possibly lead to pinwheels seen in thicker samples. Regions of near zero CD suggest the superposition of oppositely signed crystals and indicates the twinning on (001).

Lamellar twinning across (001) is most evident when a crystal is examined through the reverse side. We do not see precisely the same pattern when the wave vector is reversed. The Jones formalism for complex optical properties is consistent with this behavior, as the matrices for each layer do not commute.

### Discussion

**Enantiomorphous Twinning.** Enantiomorphous twinning in molecular crystals is rarely observed. The first example known to us comes from Goldschmidt, in 1915, who carefully examined optically active and optically inactive crystals of $\beta$-phenylglycergic acid[31] and recognized that the inactive crystals were not truly racemic but consisted of microscopic lamellae of *d* and *l* crystallites. Green and Knossow[32] observed that hexahelicene single crystals grown from racemic solutions, despite being well refined in the chiral space group $P2_12_12_1$, had upon dissolution vanishingly small optical rotations even though resolved hexahelicene has an enormous specific rotation.[33] The authors determined on the basis of the chiroptical behavior of solutions, and the lamellar texture of the crystals, that the enantiomorphous crystalline layers were interleaved. Enantiomorphic twinnings due to oscillatory crystallizations were also reported for racemic 1-(4-chlorophenyl)-4,4-dimethyl-2-(1*H*-1,2,4-triazol-1-yl)-pentan-3-one,[34] racemic 2-azabicyclo[2.2.1]-hept-5-en-3-one,[35] and racemic 5-ethyl-5-methylhydantoin.[36] The authors of these reports relied on periodic changes in the optical rotation of the crystallizing solutions and on the lamellar texture of partially dissolved crystals in making these determinations. Because enantiomorphous twins often cannot be distinguished in X-ray scattering experiments, a direct, chiroptical, solid-state assay of chiral domains was not presented in any of these cases, and we only know of their existence because the investigators were especially astute in recognizing that their crystals were other than ordinary. It must be that mirror image twinning is common but most often goes unrecognized as

(31) Goldschmidt, V. M. *Z. Kristallogr*. **1915**, *55*, 123−131. See also: Furberg, S.; Hassel, O. *Acta Chem. Scand*. **1950**, *4*, 1020−1023.
(32) Green, B. S.; Knossow, M. *Science* **1981**, *214*, 795−797. See also: Martin, R. H.; Marchant, M. J. *Tetrahedron* **1974**, *30*, 343−345.
(33) Newman, M. S.; Lednicer, D. *J. Am. Chem. Soc*. **1956**, *78*, 4765−4770.
(34) Davey, R. J.; Black, S. N.; Williams, L. J.; McEwan, D.; Sadler, D. E. *J. Cryst. Growth* **1990**, *102*, 97−102.
(35) Potter, G. A.; Garcia, C.; McCague, R.; Adger, B.; Collet, A. *Angew. Chem., Int. Ed. Engl*. **1996**, *35*, 1666−1668.
(36) Gervais, C.; Beilles, S.; Cardinaël, P.; Petit, S.; Coquerel, G. *J. Phys. Chem. B* **2002**, *106*, 646−652.

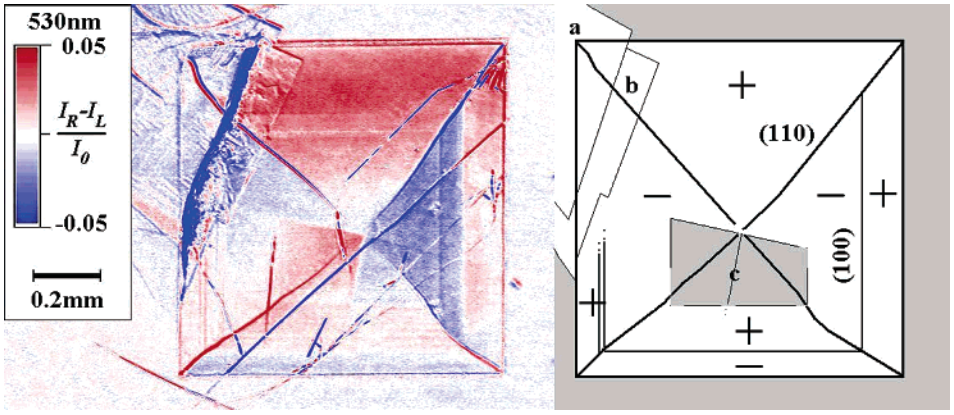


***Figure 6.*** CD micrograph at 530 nm of a thin (<50 mm) **DHA** crystal showing clearly the (110) and (100) twin planes between enantiomorphous domains. Regions a and b are thin, overlaid crystallites. Region c shows an intergrown crystal with a superposition of enantiomorphous domains ((001) twinning) that may reveal a nascent pinwheel of the kind observed in thicker samples (Figure 4e and f). The streaks are due to scratches and needles of a metastable polymorph.

evidenced by the recent report that racemic amino acids often form epitaxial lamellae of enantiomorphs.[37]

**Anomalous Birefringence.** It has been well established that strain can lead to anomalous birefringence in crystals[38] and that twinning can lead to strain. Thus, the anomalous birefringence of **DHA** may be ascribed to enantiomorphous twinning-induced strain. The regions of largest retardation at the (110) boundaries in Figure 4c are not distince in the CD image in 4e. Because the retardation is largest at the (110) boundaries and decays smoothly with distance, it most likely is caused by strain. However, the apparent changes in birefringence seen in crossed polarized light, especially in the crystal centers dominated by pinwheels, are mostly CD of **DHA** which increases the ellipticity of the transmitted light. This judgment comes from an analysis of Figure 4c and e, in which the red pinwheel (4e) shows the strongest CD and the largest sin($\delta$) (4c). Between the "red arms" the CD signal is of opposite sign but is much diminished as is sin($\delta$). Not all of the anomalous birefringence is anomalous birefringence after all.

In a grand overview of optically anomalous crystals, Brauns proposed that optical symmetry reduction could, in some crystals other than **DHA**, be a consequence of enantiomorphous twinning.[39] Until now, no evidence has been provided to support this classification.

**Absolute Configuration.** Can we assign the absolute configuration of the enantiomorphous domains as $P4_1$ or $P4_3$ directly from the CD images? Given the fact that **DHA** has spirals of intramolecular electric dipole transition moments in planes perpendicular to *c*, we might expect that the exciton chirality model would be well suited to distinguish between $P4_1$ and $P4_3$.[40] However, application of this model requires a bisignate line shape (for dimeric interactions) that is only very weakly observed in **DHA**. An alternative interpretation of the CD spectra based on charge transfer follows a discussion of the coupled oscillator model.

The **DHA** molecules in the crystal have approximate *mm*2 ($C_{2v}$) symmetry. Even if this were the site symmetry in the crystals, *mm*2 is an optically active point group[41] and individual layers could well show CD. However, an individual layer cannot contribute to the CD through the coupled dipole mechanism because the strong molecular $\pi\rightarrow\pi^*$ transition moments are all parallel.[42] The CD most likely arises from interactions of molecules between layers following the $4_{1(3)}$ axis. This interpretation is consistent with the fact that the CD signal is only associated with the shoulder in the absorption band. However, crossed dipoles typically give a bi-signate CD spectrum.[40] If the excition model is appropriate in this case, then we must conclude that the high-energy component of the excited-state split by the Davydov interaction is electric dipole disallowed. In the context of this interpretation, we reason that the $P4_1$ structure pictured in Figure 3A should give rise to a positive Cotton effect at low energy (red curve in Figure 5).

The exciton chirality method has been developed into a powerful tool for the assignment of the absolute configuration of suitably derivatized molecules in solution. This was a welcome advance because, previously, the only way to determine the absolute configuration of compounds was through the interpretation of the anomalous dispersion of X-rays, a technique notoriously unreliable for light atom organic compounds of C, H, and O, such as **DHA**. Indeed, our attempts to assign configuration with X-rays failed in the absence of a strong anomalously scattering atom. The use of the exciton chirality method to assign the absolute configuration of a crystal is rare. To the best of our knowledge, the only example comes from Aoyama and co-workers who compared the averaged CD spectra of powders of homochiral $Cd(NO_3)_2$ coordination polymers of 5-(9-anthracenyl)pyrimidine[43] with the absolute configuration determined by X-ray diffraction. Now, with the ability to measure the CD spectrum of single crystals of low symmetry directly, it should be possible to apply the exciton chirality method in the solid state with some generality, especially because the geometries of the molecules in the crystal are well defined. Conformational complexity is probably the most

(37) Berfeld, M.; Zbaida, D.; Leiserowitz, L.; Lahav, M. *Adv. Mater*. **1999**, *11*, 328−331. Weissbuch, I.; Kuzmenko, I.; Vaida, M.; Zait, S.; Leiserowitz, L.; Lahav, M. *Chem. Mater*. **1994**, *6*, 1258−1268.
(38) Nabarro, F. R. N. *Theory of Crystal Dislocations*; Dover: New York, 1987. Crundwell, G.; Gopalan, P.; Bakulin, A.; Peterson, M. L.; Kahr, B. *Acta Crystallogr., Sect. B*. **1997**, *53*, 189−202.
(39) Brauns, R. *Die Optischen Anomalien der Krystalle*; S. Hirzel: Leipzig, 1891.
(40) Harada, N.; Nakanishi, K. *Circular Dichroic Spectroscopy: Exciton Coupling in Organic Stereochemistry*; University Science Books, Mill Valley, CA, 1983.
(41) O'Loane, J. K. *Chem. Rev*. **1980**, *80*, 41−61.
(42) Madsen, F.; Terpager, I.; Olskaer, K.; Spanget-Larsen, J. *Chem. Phys*. **1992**, *165*, 351−360.
(43) Ezuhara, T.; Endo, K.; Aoyama, Y. *J. Am. Chem. Soc*. **1999**, *121*, 3279−3283.

common reason for failure of the exciton chirality method for suitably derivatized molecules in solution.[44] In crystals, we know precisely where to find the coupled oscillators.

The exciton chirality model has in the past been so compelling that researchers have used it to challenge the very foundation of the Bijvoet method.[45] Careful consideration of the transition dipoles in the puzzling ethanoanthracenes and triptycenes,[45] whose configurations determined by exciton interactions were at variance with results obtained by anomalous dispersion, dispelled the confusion.[46] However, in circumstances where the questions remain about the electronic structure of the system under investigation, past experience argues for caution. The application of the exciton chirality model in **DHA** is complicated by the fact that the excitations are undoubtedly delocalized over more than two sites.

An alternative interpretation of the CD spectrum in **DHA** relies on the assignment of the low-energy absorption as a charge transfer band between molecules in adjacent layers. In this way, there is a natural circulation of charge producing a rotary strength by the coupling of electric and magnetic dipoles. This interpretation obviates an explanation of the absence of the bisignate line shape as only a single Cotton effect would be expected. Given a helical circulation of charge in the spiral of **DHA** molecules shown in the $P4_1$ structure in Figure 3A, we would also expect parallel electric and magnetic moments and therefore a positive Cotton effect.[47]

## Conclusion

Crystals of **DHA**, large and well-formed plates, highly absorbing in the visible part of the electromagnetic spectrum, with first-order retardance ($\delta < \pi/2$), are especially well suited to CD imaging. We expect refinements in the technique will enable CD imaging of a wide range of anisotropic substances encountered in materials science and crystallography, not to mention cell biology and pathology where dyed, chiral anisotropic structures are ubiquitous. Examples of the latter are forthcoming.

While it is now beyond doubt that the weird physical properties of **DHA** first reported by Neuhaus[27] are a consequence of enantiomorphous twinning, there are many aspects of the growth of **DHA** crystals that remain to be answered: (1) What is the sense of the polar axis, and does it change between enantiomorphous domains? (2) What is the origin of the characteristic pinwheel rotation? (3) What is the origin of the CD signal? These questions drive ongoing investigations.

**Acknowledgment.** We are most grateful for the support of this work through grants from the U.S. National Science Foundation, and the Petroleum Research Fund of the American Chemical Society. E.P.-F. and M.K. received support in the form of graduate fellowships from the University of Washington Center for Nanotechnology. K.C. received the Ludo Frevel scholarship from the International Centre for Diffraction Data and a graduate fellowship from the Division of Organic Chemistry of the American Chemical Society. We thank Daniel Gamelin and Guillermo Bazan for stimulating discussions.

JA035644W

(44) Lightner, D. A.; Gurst, J. E. *Organic Conformational Analysis and Stereochemistry from Circular Dichroism Spectroscopy*; Wiley-VCH: New York, 2000.
(45) Tanaka, J.; Katayama, C. *J. Chem. Soc., Chem. Commun*. **1973**, 21−22. Tanaka, J.; Ozeki-Minakata, K.; Ogura, F.; Nakagawa, M. *Spectrochim. Acta* **1973**, *29A*, 897−924.
(46) Mason, S. F. *J. Chem. Soc., Chem. Commun*. **1973**, 239−241. Hezemans, A. M. F.; Groenewege, M. P. *Tetrahedron* **1973**, *29*, 1223−1226.
(47) Eliel, E. L.; Wilen, S. H. *Stereochemistry of Organic Compounds*; Wiley: New York, 1994; Chapter 13.